Active and Passive Elec. Comp., 1991, Vol. 14, pp. 111–118
Reprints available directly from the publisher
Photocopying permitted by license only

Printed in the United Kingdom

OPTICAL AND ELECTRICAL PROPERTIES OF SnO_2:F THIN FILMS OBTAINED BY R.F. SPUTTERING WITH VARIOUS TARGETS

C. GEOFFROY, G. CAMPET, F. MENIL, J. PORTIER
Laboratoire de Chimie du Solide du CNRS, 351 cours de la Libération, 33405 Talence (France)
J. SALARDENNE and G. COUTURIER
Laboratoire d'étude des Matériaux pour la Microélectronique, Université de Bordeaux I, 33405 Talence (France)

(Received July 10, 1990; in final form August 9, 1990)

Tin oxide films were deposited on glass substrates by reactive and non reactive r.f. sputtering using different types of targets corresponding to various Sn/F atomic ratio: hot pressed Sn–SnF_2 or SnO_2–SnF_2 mixtures, ceramics obtained by casting either an aqueous SnO_2-SnF_2 slurry or a suspension of tin oxide in molten tin fluoride. The samples were prepared in oxygen-argon gas mixtures in which the oxygen concentration was varied from 0 mole % up to 30 mole% depending on the target. The optical and electrical properties of the obtained thin films have been studied and compared to those of the films obtained by spray technique.

1. INTRODUCTION

Transparent and conductive oxide thin films have been extensively studied because of their numerous applications. In optoelectronic (solar cells) or electrochemical (smart window) devices, these materials are used as electrodes. They also are utilized as heat-reflecting filters in insulating windows or solar collectors [1].

The most studied materials are indium tin oxide (ITO), cadmium tin oxide and tin oxide doped with antimony oxide or with fluorine. Characteristics of these materials include a wide band gap and a high carrier concentration. They are also transparent to visible radiation and reflect infrared.

Among these films, tin oxide is often preferred to indium oxide for large applications because of the lower price of the metal. Doping with fluorine is more favorable than antimony, as SnO_2:F films have comparatively higher transmissions for low sheet resistances [2]. This paper is limited to the case of this material, and is referred to as "FTO".

Undoped, non-stoichiometric tin dioxide SnO_2 has a rutile type structure. It is an n-type semiconductor with a direct band gap of about 4.0 eV and an indirect band gap of about 2.6 eV [3]. Its electrical properties can be explained in two ways; the donor impurity may be connected with oxygen vacancies:

$$SnO_2 \rightleftharpoons Sn^{4+} + (2 - \varepsilon)O^{--} + \varepsilon V^{--} + \varepsilon/2O_2 \quad (1)$$

(V represents vacancies in the anionic lattice)

or with interstitial tin atoms [4]:

$$SnO_2 \rightleftharpoons (1 - \varepsilon)Sn^{4+} + \varepsilon Sn^0 + (2 - 2\varepsilon)O^{--} + \varepsilon O_2 \quad (2)$$

When doped with fluorine, tin dioxide become a degenerate semiconductor. The mechanism of formation of donors could be [5]:

$$xF^- + x\,e^- + SnO_2 \rightleftharpoons (Sn^{4+} + xe^-)F_xO_{2-x} + x\,O^{--} \quad (3)$$

Consequently, for each fluorine ion, an electron is introduced into the conduction band.

FTO films are generally prepared either by a chemical spray method or by chemical vapor deposition. In both cases, the starting materials are stannic chloride or tin organometallic compounds [1]. Both processes involve a strong reducing medium at relatively high temperatures ($T > 400°C$). These conditions make the film preparation dangerous when used for coating large glass surfaces. Consequently, it is important to investigate other methods.

The purpose of this study was to evaluate r.f. sputtering as a method of preparing FTO films. In a first part, we have studied the fabrication of targets with $Sn–SnF_2$ or $SnO_2–SnF_2$ mixtures. The electrical and optical properties have been investigated and correlated with the composition of the target and the sputtering conditions, and compared to those of films obtained by the spray method.

2. TARGET FABRICATION

Tin difluoride was to combine fluorine atoms and tin in its lower oxidation state. This compound melts uncongruently at 216°C:

$$2\,SnF_2 \rightleftharpoons Sn + SnF_4 \quad (4)$$

When the melting is done under an oxidizing and humid atmosphere, various oxidation and hydrolysis reactions occur:

$$SnF_2 + H_2O \longrightarrow SnO + 2\,HF \quad (5)$$

$$SnF_4 + 2\,H_2O \longrightarrow SnO_2 + 4\,HF \quad (6)$$

$$Sn + 1/2\,O_2 \longrightarrow SnO \quad (7)$$

$$SnO + 1/2\,O_2 \longrightarrow SnO_2 \quad (8)$$

At 800°C, the last term is tin dioxide.

For this study metallic tin powder (Aldrich, purity 99.8%), tin difluoride (Cerac, purity 99.9%), and tin dioxide (Aldrich, purity 99.8%) have been used.

2.1. *Sn–SnF_2 Target*

Powders of tin metal and difluoride were co-melted at 240°C and poured into a mould (Cerac-Neyco). This target will be called Type I.

2.2. *SnO_2–SnF_2 Targets*

Taking into account the chemical reactions described above, the evolution of the fluorine content with preparation conditions was studied. Four targets were annealed at 260°C for four hours. The composition was determined by gravimetric analysis on the basis of the above reactions. After annealing, a piece of target was treated by nitric acid in order to oxidize all divalent tin and then calcined at 1000°C. from the weight of tin dioxide, it is possible to know the fluorine content after annealing. The results are compiled in Table I.

On the basis of these results three types of targets were prepared:

i) Type II. Several targets were obtained by hot pressing under argon in a graphite mould of mixtures of x% SnF_2 − (100 − x)% SnO_2 (T°C = 260; x = 3, 5, 10).

ii) Type III. Another target was obtained as follows: a mixture was prepared by adding to molten SnF_2 a specific amount of SnO_2 in order to obtain a paste, which was then poured into a mould. To minimize the proportion of difluoride, the surface of the target was sprinkled before solidification with fine tin dioxide powder. This last method is easy to operate and can be used to prepare targets with a large diameter. However, it is difficult to know exactly the O/F ratio in the target.

iii) Type IV. An aqueous SnO_2–SnF_2 slurry was obtained by adding to a given amount of tin dioxide a solution of tin difluoride in water. This slurry was poured in a mould, slowly dried under an infrared lamp, and heated during four hours at 260°C. This method yields a target with a controlled O/F ratio. However, targets with a large diameter (>5 cm) are difficult to obtain without cracks.

3. THIN FILMS

Thin films were deposited on glass substrates from four targets, corresponding to the four types previously described, using RF sputtering equipment (Alcatel).

TABLE I
Evolution of target composition after annealing at 260°C during four hours.

Before annealing			After annealing		
SnF_2 wt%	F/Sn atom.	O/Sn atom.	SnF_2 wt%	F/Sn atom.	O/Sn atom.
5	0.10	1.9	3	0.06	2.02
10	0.19	1.8	8.1	0.16	1.85
15	0.29	1.71	10.2	0.20	1.85
20	0.39	1.61	16.9	0.33	1.68

TABLE II
Sputtering parameters corresponding to the four used targets.

Target	Target composition	Power (W)	Gas pressure mb	Gas composition %	Substrate temperature °C
Type I	95% Sn 5% SnF_2	40	$5\ 10^3$	Ar 70 O_2 30	25
Type II	90–98% SnO_2 10–2% SnF_2	50	$5\ 10^3$	Ar 100	450
Type III	50% SnO_2 50% SnF_2	50	$5\ 10^3$	Ar 95 O_2 5	450
Type VI	90% SnO_2 10% SnF_2	50	$5\ 10^3$	Ar 100	450

Various sputtering parameters were used depending on the type of target. They are shown in Table II, and correspond to the conditions leading to the highest performances of the films.

3.1. Thin Film Composition

The chemical composition has been studied in the case of the films obtained with targets of type II and III. The films were deposited on a polished carbon substrate. Because of the unaccuracy of fluorine analysis by methods using electron or ionized particles [7], we used Rutherford Back Scattering [6] for the determination of the amount of fluorine ions in the films. The results are shown in Table III. It is noted that the F/Sn ratio is about ten times lower in the film than in the target. The fluorine concentration reaches 2.05×10^{21}at.cm^{-3} in samples I and II of Table III. This value is comparable to that obtained with sprayed SnO_2:F films (1.6×10^{21} at. cm^{-3}) [7].

The composition of a type II target was determined after sputtering by chemical analysis (Service Central D'analyse du CNRS) (Table IV). The ratio ($F_{surface}/F_{bulk}$) (at.%) is equal to 0.5, showing that the fluorine content is decreased at the surface indicating a preferential etching of fluorine ion as a consequence of the ionic Sn–F bonding weaker than the more covalent Sn–O bonding.

TABLE III
Fluorine content of some films obtained with a target with composition 0.9 SnO_2-0.1 SnF_2 with argon plasma (p = 0.3 bar).

Sample	Deposition time h	Power (W)	Thickness Å	F/Sn at. ± 0.2	O/Sn at. ± 0.1
1	2	15	1670	0.08	1.95
2	2	26	2500	0.08	1.8
3	1	30	1950	weak	1.83

3.2. Structure and Texture

For all the targets the obtained films are amorphous when the substrate is cold. Crystalline films are obtained when the substrate is heated in-situ above 450 C. X-ray diffractometry shows that the only observed phase is SnO_2 cassiterite type. In all cases a preferential orientation is observed depending on the thickness. For films thinner than 3000 Å, an orientation along the [110] is observed; thicker films are orientated along [101] (Fig. 1). Such a phenomenon has already been observed for sprayed SnO_2:F films [7].

Amorphous samples obtained on cold substrates were annealed at 450°C for several hours under air or vacuum (2×10^5mbar). They recrystallized with a [110] preferential orientation, independent of their thickness.

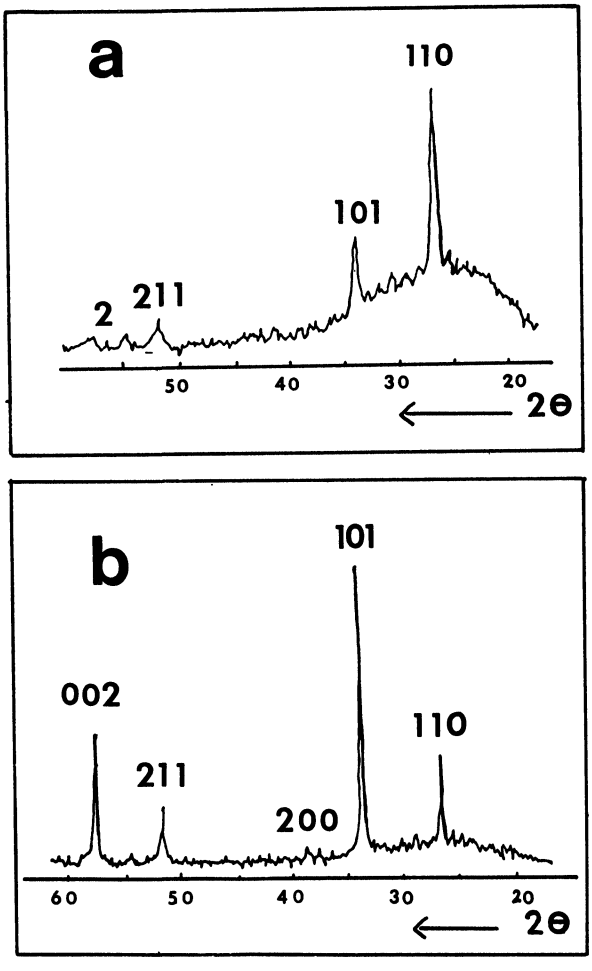

FIGURE 1 X-ray diagrams (Cu Kα radiation) of SnO_2:F; a) e = 2500 Å; b) e = 6100 Å.

Two types of texture were observed by electron microscopy; spherical grains and columns. It is difficult to associate the shape of the grain with the crystallinity. In general, however, amorphous and thin films (e < 2000 Å) are granular when crystalline and thick films (e > 2000 Å) are composed of columns. The best electrical performances are obtained in the second case.

3.3. Optical properties

The optical properties were measured for three films deposited from a type II target. Transmittance (T) and reflectance (R) were recorded using a Beckman a DK-2A spectrophotometer from 400nm to 2500nm (Fig. 2).

The direct and indirect optical band gap are, respectively, 3.8 eV and 2.6 eV in agreement with the previous studies.

T_{max} reaches about 90% at 500–700 nm, higher than that of films obtained by spray or CVD techniques. Indeed, with these methods it is more difficult to control the oxidation-reduction conditions, and very often traces of black SnO are obtained leading to a reduced transmission [1, 8]. In contrast, R is relatively low (T_{2500nm} = 50–25% for in-situ crystallized films; 16% for amorphous or ex situ crystallized films), and is approximately two times less than that of films prepared by spray [1].

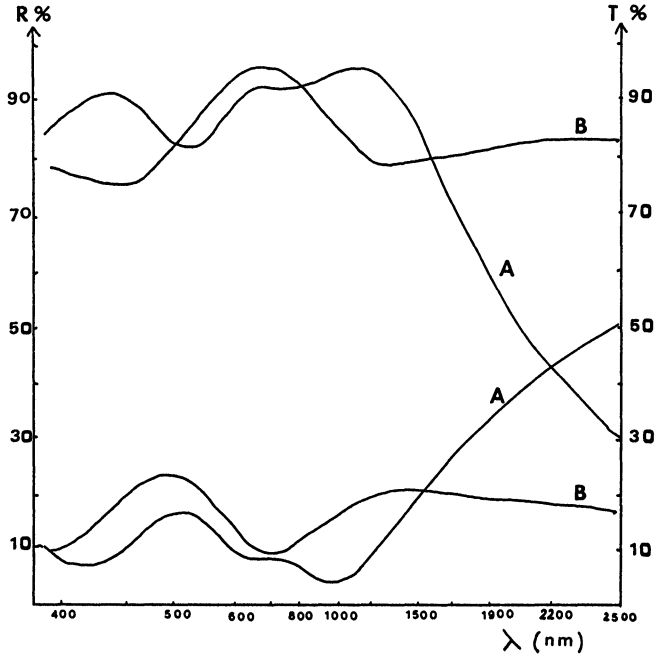

FIGURE 2 Transmittance and reflectance vs. wavelength for SnO_2:F films obtained with a type II target (A crystallized, e = 2000 Å; B amorphous, e = 3500 Å).

3.4. Electrical Properties

From measurements at room temperature of the Hall constant and of the d.c. conductivity (four points method), the carrier concentration N, the carrier mobility μ, and the sheet resistance $R_\square$ were measured.

The electrical properties obtained with the four types of target are shown in Table IV. The highest conductivity was obtained with a type II target. The corresponding sheet resistance is $R_\square = 25\ \Omega/_\square$, associated with a 90% transmission at 500–700 nm. This value can be compared to the best performance obtained with sprayed FTO films (9.2 $\Omega/_\square$ with $T_{650nm} = 93\%$ [9]).

From Hall measurements on a freshly prepared film (target type II) we observed a number of carriers of 7×10^{20} cm^{-3} associated with a carrier mobility of 25 $cm^2V^{-1}s^{-1}$. These results are close to those obtained by spray deposition by Fantini and Torriani [7] ($n_H = 10^{18}$–10^{20} cm^{-3}; μ_H = 6–44 $cm^2V^{-1}s^{-1}$. The number of carriers can be compared to the number of fluorine atoms (2.05×10^{21}at.cm^{-3}). Because of the inaccuracy of the RBS analysis one can conclude to a reasonable agreement.

3.5. Film Aging

After six months' aging, the previous sample had very different characteristics. Indeed n_H had decreased from 7×10^{20} to 10^{19} cm^{-3} and μ_H from 25 to 4 $cm^2V^{-1}s^{-1}$. A possible explanation could be the adsorption of oxygen at grain boundaries. This adsorption is particularly easy with films with a column type texture. Indeed, it is well known that tin dioxide is very sensitive to oxidizing or reducing species; this property is used in chemical sensors [10]. In the case of FTO films the following aging mechanism can be proposed. The oxygen from the surrounding atmosphere is physisorbed on the surface of the FTO grains. Free electrons could then react to form superoxide ions as follows:

$$\varepsilon\ O_2 + 2\varepsilon\ e^- \longrightarrow \varepsilon\ O_2^{--} \tag{9}$$

This reaction would lead to a lowering of the number of free carriers and also to a decrease of the mobility, especially at the grain boundaries.

To verify the previous hypothesis, an aged sample was treated for two hours at room temperature under an argon-fluorine atmosphere (Ar 90%, F_2 10%). The

TABLE IV
Optimized resistivity of FTO films obtained with various targets.

Target types	ρ Ω cm	$R_\square$ Ω
I	2×10^{-1}	700
II	5×10^{-4}	25
III	10^{-3}	40
IV	5×10^{-3}	200

resistivity immediately decreased probably due to a reinjection of electrons into the semiconductor conduction band following the reaction:

$$\varepsilon\, O_2^{--} + 2\varepsilon\, F_2 \longrightarrow 2\varepsilon\, F_2O + 2\varepsilon\, e \qquad (10)$$

4. CONCLUSION

In this work we have demonstrated that RF sputtering from fluorine-containing targets can be used to produce FTO films with optical and electrical performances comparable to those of films produced by spray or CVD techniques. However, the preferential etching of fluorine ions leads to a rapid evolution of the composition of the surface of the target. This behavior makes the reproducibility of the films difficult. In addition, the texture of crystalline films made of columns permits the penetration of atmospheric oxygen in the bulk of the films leading to the formation of peroxide ions, thereby lowering the number of free electrons. The consequence is a rapid aging of the films.

ACKNOWLEDGMENT

We are grateful to GRL (Elf-Aquitaine) for financial support. We thank Dr. R. Panaras (GRL), Dr. J.P. Couput (GRL), Pr. J.B. Goodenough and Dr. R. Castellano for their interest in the subject.

REFERENCES

1. K.L. Chopra, S. Major and D.K. Pandya, Thin Solid Films, 102 (1983) 1.
2. A. Bhardwaj, B.K. Gupta, A. Raza, A.K. Sharma and O.P. Agnihotri, Solar Cells (1981–1982) 39.
3. A.K. Saxena, R. Thangaraj, S.P. Singh and O.P. Agnithotri, Thin Solids Films, 131 (1985) 121.
4. E. Leja, J. Korecki, K. Krop and K. Toll, Thin Solids Films, 59 (1979) 147.
5. C.M. Lampert, Ind. Eng. Chem. Prod. Res. Dev. 21 (1982) 612.
6. L.C. Feldman and S.T. Picraux in "Ion beam handbook for material analysis", eds. J.W. Mayer and E. Rimini, Academic Press, New York (1977) 166–9.
7. M. Fantini and I. Torriani, Thin Soids Films, 138 (1986) 255.
8. A.K. Saxena, R. Thangaraj, S.P. Singh and O.P. Agnihotri, Thin Solids Films, 131 (1985) 121.
9. E. Shanti, A. Banerjee and K.L. Chopra, J. Appl. Phys., 51 (1980) 6243.
10. G. Heiland, Sensors and Actuators, 2 (1982) 343.

EURASIP Journal on Image and Video Processing

Special Issue on Dependable Semantic Inference

Call for Papers

After many years of exciting research, the field of multimedia information retrieval (MIR) has become mature enough to enter a new development phase—the phase in which MIR technology is made ready to get adopted in practical solutions and realistic application scenarios. High users' expectations in such scenarios require high dependability of MIR systems. For example, in view of the paradigm "getting the content I like, anytime and anyplace" the service of consumer-oriented MIR solutions (e.g., a PVR, mobile video, music retrieval, web search) will need to be at least as dependable as turning a TV set on and off. Dependability plays even a more critical role in automated surveillance solutions relying on MIR technology to analyze recorded scenes and events and alert the authorities when necessary.

This special issue addresses the dependability of those critical parts of MIR systems dealing with semantic inference. Semantic inference stands for the theories and algorithms designed to relate multimedia data to semantic-level descriptors to allow content-based search, retrieval, and management of data. An increase in semantic inference dependability could be achieved in several ways. For instance, better understanding of the processes underlying semantic concept detection could help forecast, prevent, or correct possible semantic inference errors. Furthermore, the theory of using redundancy for building reliable structures from less reliable components could be applied to integrate "isolated" semantic inference algorithms into a network characterized by distributed and collaborative intelligence (e.g., a social/P2P network) and let them benefit from the processes taking place in such a network (e.g., tagging, collaborative filtering).

The goal of this special issue is to gather high-quality and original contributions that reach beyond conventional ideas and approaches and make substantial steps towards dependable, practically deployable semantic inference theories and algorithms.

Topics of interest include (but are not limited to):

- Theory and algorithms of robust, generic, and scalable semantic inference
- Self-learning and interactive learning for online adaptable semantic inference
- Exploration of applicability scope and theoretical performance limits of semantic inference algorithms
- Modeling of system confidence in its semantic inference performance
- Evaluation of semantic inference dependability using standard dependability criteria
- Matching user/context requirements to dependability criteria (e.g., mobile user, user at home, etc.)
- Modeling synergies between different semantic inference mechanisms (e.g., content analysis, indexing through user interaction, collaborative filtering)
- Synergetic integration of content analysis, user actions (e.g., tagging, interaction with content) and user/device collaboration (e.g., in social/P2P networks)

Authors should follow the EURASIP Journal on Image and Video Processing manuscript format described at http://www.hindawi.com/journals/ivp/. Prospective authors should submit an electronic copy of their complete manuscripts through the journal Manuscript Tracking System at http://mts.hindawi.com/, according to the following timetable:

Manuscript Due	November 1, 2008
First Round of Reviews	February 1, 2009
Publication Date	May 1, 2009

Guest Editors

Alan Hanjalic, Delft University of Technology, 2600 AA Delft, The Netherlands; a.hanjalic@tudelft.nl

Tat-Seng Chua, National University of Singapore, Singapore 119077; chuats@comp.nus.edu.sg

Edward Chang, Google Inc., China; University of California, Santa Barbara, CA 93106, USA; echang@ece.ucsb.edu

Ramesh Jain, University of California, Irvine, CA 92697, USA; jain@ics.uci.edu